

Red QSOs in the M_{BH} - M_* plane

Angela Bongiorno

INAF, Osservatorio Astronomico di Roma,
via di Frascati 33, Monteporzio Catone - Rome, Italy
email: angela.bongiorno@oa-roma.inaf.it

Abstract. We present new results on the the M_{BH} - M_* relation of X-ray obscured, red QSOs at high redshift ($1.2 < z < 2.6$). The sample is made of 21 red QSOs, nine of them are new sources for which near-infrared spectra have been obtained with SINFONI and XShooter observations at ESO VLT, and show a broad $H\alpha$ component. The rest of the sample (12 sources) is made of sources taken from the literature with similar properties. From the broad $H\alpha$ line we have computed the BH masses through the virial formula while stellar masses have been obtained through multi-component SED fitting.

We find that red QSOs preferentially lie on the local relation up to $z \sim 2.6$ with the most massive objects mainly located above it. We also studied the evolution of these sources on the M_{BH} - M_* plane compared to a sample of optically blue type-1 QSOs and we find that obscured red QSOs show a constant M_{BH}/M_* ratio consistent/slightly higher than the local one but lower than what has been found for blue QSOs. These sources may represent the intermediate phase (blow-out phase) between the major-merger induced starbursts which appear as ULIRGs and SMGs and the optical type-1 blue QSOs which are revealed once the dust and nuclear gas is cleared up.

1. Introduction

The discovery of a tight local correlation between the mass of Supermassive Black Holes (SMBHs) and the stellar and dynamical mass of their host spheroids, the two having a mass ratio $M_{BH}/M_* \sim 10^{-3}$ over several orders of magnitudes in mass, constitutes an important breakthrough in the understanding of galaxy evolution, implying that a strong physical connection exists between galaxy formation and the growth of black holes at their centers (e.g. Magorrian *et al.* 1998; Marconi & Hunt 2003).

At high redshift, most studies have focused on optically blue type-1 broad line AGN (BLAGN) (e.g. Peng *et al.* 2006; Merloni *et al.* 2010; Salvander & Shields 2013) for which the UV broad lines (e.g. MgII and CIV, observed in the optical band at high- z) are detected and hence virial formulas can be used to derive BH masses from the AGN luminosity and the width of the broad lines. New important constraints in understanding the physical nature of the AGN-galaxy coupling require the extension of the analysis of the BH-galaxy relation to the population of X-ray obscured, dust reddened QSOs. Dusty broad-line quasars could represent galaxies caught in a very interesting phase of the AGN life, i.e. the blow-out phase. During this moment, we expect the central source to be buried by the surrounding material and the AGN to likely appear as an optically type-2 AGN, X-ray obscured and red.

2. The sample

We have obtained new IR spectra with SINFONI and XShooter at ESO VLT of 9 X-ray obscured, red ($R-K > 5$) QSOs for which a broad $H\alpha$ component has been observed in the IR spectra. We complement these data with additional sources taken from the literature

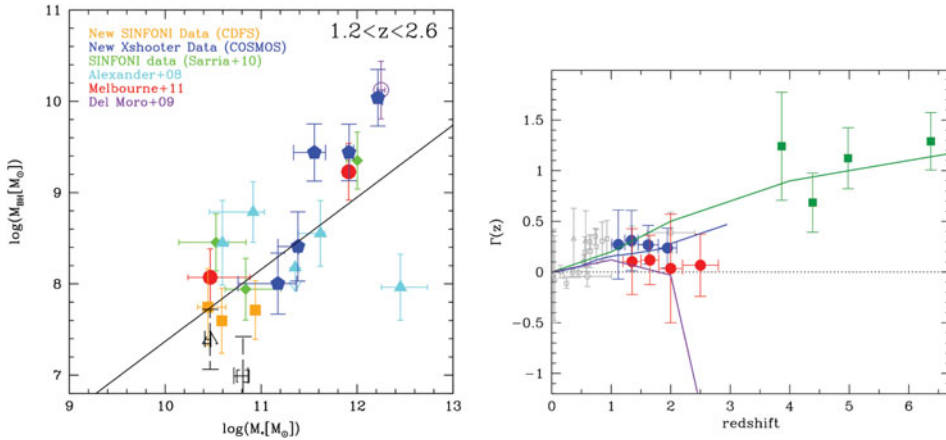


Figure 1. *Left:* Scaling relation between M_{BH} and M_* for obscured AGN at $z \sim 1.2 - 2.6$ color-coded as explained in the inset of the plot. The solid line is the local relation from Sani *et al.* (2011). *Right:* Binned average offset (and its dispersion) $\Gamma(z)$ from the local M_{BH} - M_* relation for our sample (red circles), the comparison sample (blue circles and grey symbols), and high-redshift massive QSO (green squares), compared with the paths in the $M_{BH}(t)$ - $M_*(t)$ plane followed, during their evolution, by BHs and their host galaxies according to the semi-analytical model by Menci *et al.* (2008).

with similar properties, reaching a final total sample of 21 X-ray obscured, intermediate type, red QSOs with broad $H\alpha$ emission. This represents the most extensive study so far for this class of targets. As a comparison sample, we considered the sample of 90 unobscured, optically type-1, blue QSOs (R-K \sim 2-3) from the zCOSMOS survey in the redshift range $1 < z < 2.2$ presented in Merloni *et al.* (2010).

3. The M_{BH} - M_* scaling relation

In the left panel of Fig. 1, we show the M_{BH} - M_* plane. Different symbols and colors show the collected samples which span the $z \sim 1.2 - 2.6$ range; the solid line is the local relation from (Sani *et al.* 2011) taken as reference.

We find that, X-ray obscured, red QSOs are largely scattered but they mostly lie on the local scaling relation. In particular, while less massive objects are equally scattered below and above the local relation, the most massive ones are mainly found above.

Evolution of the M_{BH} - M_ scaling relation*

In the right panel of Fig. 1, we plot in redshift bins, the average values and dispersions of the offset $\Gamma(z)$ between the M_{BH}/M_* and the local values, calculated as distance in the log space of each point to the Sani *et al.* (2011) correlation: $\Gamma(z) = \log(M_{BH}/M_*)(z) - \log(M_{BH}/M_*)(z = 0)$. Red circles are the average values and dispersions of our data binned in four redshift bins while the blue circles are for the blue QSOs from Merloni *et al.* (2010). Grey open symbols are objects from literature (Salviander *et al.* 2007; Shields *et al.* 2003; Woo *et al.* 2008; Peng *et al.* 2006). We also show some extreme objects i.e. massive BHs already in place at high redshifts (green squares, Maiolino *et al.* 2007). While blue QSOs show M_{BH}/M_* ratios increasing going to earlier epochs (Peng *et al.* 2006; Maiolino *et al.* 2007; Merloni *et al.* 2010), red QSOs show on average a constant ratio up to high redshift ($z \sim 2.6$) i. e., slightly higher than local but lower than the one found for blue QSOs.

In the same figure we overplot the evolutionary tracks in the $M_{BH}(t)-M_*(t)$ plane predicted from the semi-analytical model of Menci *et al.* (2008) considering sources with different selection criteria. The two extreme cases are represented by the green and violet tracks. The green one corresponds to the evolution of the massive QSOs already in place at $z>4$ while the violet line denotes highly star-forming, dust obscured SMGs observed at $z=2-3$. Finally the blue line is for less extreme objects i.e. optical blue QSOs observed at intermediate redshift. In the model, the evolution is basically driven by the relative predominance of the two acting processes: (i) interactions (major mergers, minor mergers and fly-by) which trigger both starburst events and SMBH growth by inflow of cold gas. During these events, both the BH and the galaxy increase their mass, with the BH at a higher rate and (ii) quiescent star formation corresponding to the gradual conversion of gas into stars which is always ongoing and responsible for the galaxy growth. Depending on the process that dominates at a life stage, AGN will then move in the $\Gamma(z) - z$ plane. Massive QSOs already in place at $z>4$ have formed in biased regions of the density field where the number and the effectiveness of high-redshift interactions are responsible for assembling such huge BH masses so early in the evolution. Going to lower redshift, the number of interactions decreases causing a smaller BH mass growth compared to the galaxy mass growth which starts being dominated by the quiescent SF. For these kinds of objects, $\Gamma(z) > 0$ holds at any time between $z = 6$ and the present but the ratio M_{BH}/M_* slowly decreases going to lower redshift converging towards the local relation at $z=0$. The same happens to less extreme objects i.e. optical QSO at $z\sim 2$ with lower luminosity compared to the high redshift massive QSO. These objects originate from merging histories characterized by a lower rate of high redshift encounters and therefore show a lower excess in $\Gamma(z)$. On the contrary, selecting SMGs at $2 < z < 3$, i.e. objects with high gas fraction and high star formation rate at $z\sim 2$, we look at galaxies originated from much more quiet merging histories so that a large fraction of gas is still available at lower redshifts. Since in the semi-analytical model, high-redshift interactions are the only trigger for early BH growth, this results in low values of $\Gamma(z)$ (< 0) at $z>2$. These objects are strongly interacting at $2 < z < 3$ and therefore their BH will grow much faster than their galaxy mass going to lower redshift. They will then end up in lower redshift ($z<2$) descendants which lie on the local $M_{BH}-M_*$ relation.

In this theoretical framework, the position of X-ray obscured, dust reddened QSOs can be interpreted in different ways (Fig. 2 shows a schematic view of the proposed models):

(i) dust reddened and blue QSOs are the same population and they thus do not represent different phases in the AGN lifecycle. The fact that X-ray obscured, red QSOs are found below the blue ones can be explained considering that they are hosted in galaxies with a relatively large amount of gas and dust which indicates that these galaxies have not undergone many merging events in the past thus retaining most of their gas. This means that the BHs at the center of these sources didn't grow much compared to the corresponding optical blue QSOs in the same redshift range. On the contrary, even without merging events, the galaxy can grow through quiescent star formation resulting, on average, in lower M_{BH}/M_* ratios. According to this interpretation the path followed by red QSOs would be similar to the one drawn for blue QSOs but slightly lower i.e. they reach and settle into the local relation from above ($\Gamma > 0$).

(ii) An alternative interpretation is that these sources may represent an intermediate phase (blow-out phase, see e.g. Hopkins *et al.* 2008) between the major-merger induced starbursts which appear as ULIRGs and SMGs and the optical type-1, blue QSOs which are revealed once the dust and nuclear gas is cleared up. This can be roughly quantified using the semi-analytical model from Menci *et al.* (2008) and looking at the progenitors of $z\sim 1.5$ obscured reddened QSOs. We find that it is ten times more probable that an SMG

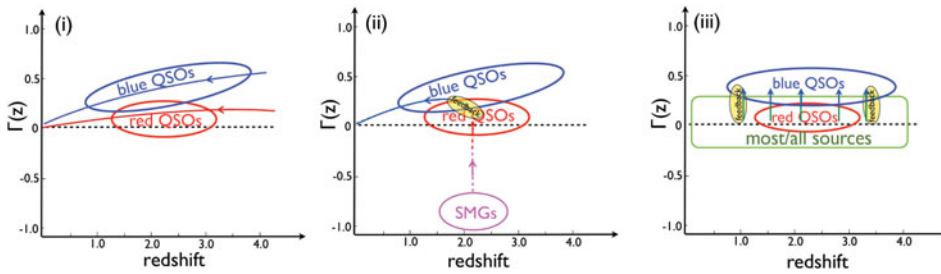


Figure 2. Schematic view of the three evolutionary scenarios proposed to explain the location of red and blue QSOs in the $\Gamma(z) - z$ plane.

will evolve in a red QSO than in an optical blue QSO. According to this interpretation, the path followed by red QSOs would be the same as the violet line in Fig. 1 (right panel), i.e. they reach and settle into the local relation from below ($\Gamma < 0$).

(iii) Finally, a much simpler scenario can be foreseen in which, for the majority of the sources, the local scaling relation holds up to high redshift and describes the secular BH-galaxy co-evolution along the cosmic time. On top of this average behavior, for a subsample of these sources, an increase of the interactions causes an anomalous BH accretion moving these objects above the local relation. In this scenario, we would thus expect X-ray obscured sources, which represent the majority of the AGN population, to lie along the local relation up to high redshift. On the contrary, the outliers busted above the relation would be able to clean up the region around the BH and they would then show up for a short phase as unobscured blue QSOs.

An additional information can be obtained looking at the SFRs and Eddington ratios of the sources. We find that 80% of the BHs are accreting at $\lambda > 10\%$ and, most of them (70%) are hosted in starburst/main sequence galaxies. This is in agreement with the interpretation (ii) i.e. these sources are caught during the blow-out phase during which we expect high SFRs.

References

- Hopkins, P. F. *et al.* 2008, *ApJS*, 175, 356
 Magorrian, J. *et al.* 1998, *AJ*, 115, 2285
 Maiolino, R. *et al.* 2007, *A&A*, 472, L33
 Marconi, A. & Hunt, L. K. 2003, *ApJ (Letters)*, 589, L21
 Menci, N., *et al.* 2008, *ApJ*, 686, 219
 Merloni, A. *et al.* 2010, *ApJ*, 708, 137
 Peng, C. Y. *et al.* 2006, *ApJ*, 640, 114
 Salviander, S. & Shields, G. A. 2013, *ApJ*, 764, 80
 Salviander, S. *et al.* 2007, *ApJ*, 662, 131
 Sani, E. *et al.* 2011, *MNRAS*, 413, 1479
 Shields, G. A. *et al.* 2003, *ApJ*, 583, 124
 Woo, J. *et al.* 2008, *ApJ*, 681, 925